

Seismo-ionospheric anomalies and implications from recent GNSS observations in India and South-East Asia

C.D. Reddy*

Indian Institute of Geomagnetism, Navi Mumbai, India

ARTICLE INFO

Article history:

Received 23 November 2015

Accepted 6 January 2016

Available online xxx

Keywords:

Earthquake

Tsunami

Ionosphere

GNSS

TEC

ABSTRACT

The lithosphere and the atmosphere/ionosphere, continuously exchange energy through various coupling mechanisms. Earthquake creates waves of energy, e.g. direct shock acoustic waves (SAWs) and Rayleigh wave induced acoustic waves (RAWs). In the event of an earthquake occurring beneath the sea, atmospheric gravity waves (AGWs) are also generated. If the earthquake is large enough ($M_w > 6$), SAWs, RAWs and AGWs induce detectable ionospheric plasma perturbations. Inferring the seismological information from these seismo-ionospheric manifestations is the subject that pertains to ionospheric seismology. Both ground and satellite based advanced radio techniques are being used in monitoring ionospheric plasma perturbations. In this study, seismo-ionospheric anomalies and implications from recent GNSS observations in India and South-East Asia are discussed, mainly pertaining to the following. (1) From the ionospheric plasma response to 2015 Nepal earthquake, the estimated group velocity for Andaman and Indian shield regions are 2100 ms^{-1} and 3900 ms^{-1} respectively and validated from ground measurements. (2) Atmospheric acoustic resonance at 4.0 mHz and a train of wave packet of TEC variation resulting from the beat phenomenon observed at the site 'umlh' and (3) GNSS-based tsunami warning which is going to be promising tool in augmenting the existing tsunami warning systems.

© 2016, Institute of Seismology, China Earthquake Administration, etc. Production and hosting by Elsevier B.V. on behalf of KeAi Communications Co., Ltd. This is an open access article under the CC BY-NC-ND license (<http://creativecommons.org/licenses/by-nc-nd/4.0/>).

* Corresponding author.

E-mail address: cdrreddy@iigs.iigm.res.in (C.D. Reddy).

Peer review under responsibility of Institute of Seismology, China Earthquake Administration.



Production and Hosting by Elsevier on behalf of KeAi

<http://dx.doi.org/10.1016/j.geog.2016.03.006>

1674-9847/© 2016, Institute of Seismology, China Earthquake Administration, etc. Production and hosting by Elsevier B.V. on behalf of KeAi Communications Co., Ltd. This is an open access article under the CC BY-NC-ND license (<http://creativecommons.org/licenses/by-nc-nd/4.0/>).

Please cite this article in press as: Reddy CD, Seismo-ionospheric anomalies and implications from recent GNSS observations in India and South-East Asia, *Geodesy and Geodynamics* (2016), <http://dx.doi.org/10.1016/j.geog.2016.03.006>

1. Introduction

Ionospheric disturbances are caused from sources located above it, e.g. the sun, interplanetary medium, magnetosphere, and below it, e.g. mesosphere, stratosphere, troposphere and lithosphere. Lithospheric disturbances are mainly due to earthquakes, volcanic eruptions, cryospheric or human activity (e.g. nuclear explosions). Following an earthquake, the ionosphere is mainly disturbed by shock acoustic waves (SAW), Rayleigh wave (surface seismic wave) induced acoustic waves (RAW) and tsunami induced gravity waves (AGW) whose frequencies fall between 0.1 mHz and 10 mHz. Detecting these seismo-ionospheric signals turns out to offer a possible remote sensing of seismic signals [1] mainly for two reasons (1) by continuity of vertical displacement at the surface, the atmosphere is then forced to move with the same vertical velocity as the ground surface and (2) conservation of kinetic energy and the exponential decrease of air density with the height. Further, it should be noted that it is easier to detect waves propagating in ionospheric plasma, more than in neutral atmosphere because of the radio-propagation properties (dispersive nature) of plasma.

The recent technological advances colossally facilitating the monitoring of seismo-ionospheric perturbations with both ground and space based advanced radio techniques. HF Doppler sounding [2,3], DEMETER [4], Over-The-Horizon radar [5,6], and Global Navigation Satellite Systems (GNSS) [7–10] are some of the well-established techniques for monitoring ionospheric plasma perturbations caused by large earthquakes. In particular, the GNSS receivers are very handy and affordable and provide integrated Total Electron Content (TEC, $1 \text{ TECU} = 10^{16} \text{ ele/m}^2$). GNSS-based ionospheric measurement can measure TEC variations smaller than 0.01 TECU [11]. It should be noted that the terms Global Positioning System (GPS) and GNSS are synonymously used.

It is demonstrated that, in the Asian region, dense GNSS arrays such as Japanese GPS Earth Observation Network (GEONET), operated by GSI, Japan [3], Sumatra GPS Array (SuGAR), Indian Seismic and GPS Network (ISGN) [9], Nepal GPS Network (NGN), Crustal Movement Observatory Network of China (CMONOC) etc. provide an opportunity to investigate ionospheric perturbations and their spatio-temporal characteristics. Jin et al. [12] and Occhipinti [13]

provide very good review on GNSS ionospheric seismology and some recent observation evidences and characteristics based on high dense GNSS network data. The imaged ionospheric perturbations from dense GPS arrays could, in principle, be used as a proxy to study the coupling and energy transfer processes in the Lithosphere, Atmosphere and Ionosphere (LAI) coupled system and earthquake source mechanism characteristics. Even more, it is very important and interesting to study any traces of precursory anomalies (from an earthquake preparation zone) in LAI coupled system [14].

Large earthquakes are most common in areas of subduction (e.g. subduction of the Pacific plate beneath the Philippine Sea plate) and convergence (e.g. India and Eurasia collision, Himalaya region) zones. The South-East Asia region is a tectonically active and most affected by highly destructive eruptions from volcanoes, devastating earthquakes and tsunamis due to its unique geological location, e.g. its proximity to the Ring of Fire. Some of the large earthquakes occurred in this region are 2011 Mw 9.0 Tohoku-Oki and 2004 Mw 9.2 Sumatra, following tsunamis, inflicted an imaginable destruction for life and property. Some of the events above Mw7.8 since 2004 are listed in Table 1. From the Table 1, though it is seen that the ionospheric response to larger earthquakes is seen pronounced in general, it should be noted that the TEC response also depends on the earthquake mechanism (strike slip, thrust etc.), time of the earthquake, proximity to the equator, the solar activity etc. All these earthquakes facilitated to study the near and far field ionospheric perturbations and also information on earthquake mechanism, fault rupture, radiation pattern etc. In this paper we address some of the societal implications such as delineating the Rayleigh group velocity and augmentation of the tsunami warning system, from the GPS data collected by many GNSS networks operating in above-said regions.

2. GPS data analysis

We used GPS data from International GNSS Service (IGS) [17], Integrated Seismic and GPS Network (ISGN), Nepal GPS Network (NGN), Sumatra GPS Array (SuGAR). Compounding all these networks, we obtained an excellent GPS data set to study the

Table 1 – Earthquakes with Mw > 7.8 that occurred since 2004 causing significant ionospheric perturbations (based on Cahyadi [15,16]).

Event	Date	Mw	Lon (°E)	Lat (°N)	Depth	Uplift	TECU
Sumatra	Dec. 26, 2004	9.2	95.41	9.37	30 km	3.4 m	6.6
Tohoku-Oki	Mar. 11, 2011	9.0	141.87	37.38	24	5.0	4.2
Nias	Mar. 28, 2005	8.6	97.013	2.074	30	2.0	>10*
Indian-Ocean	Apr. 11, 2012	8.6	93.48	7.19	23	2.1	2.6
Bengkulu	Sep. 12, 2007	8.5	101.374	-4.520	34	1.3	6.1
Indian-Ocean	Apr. 11, 2012	8.2	92.01	4.08	16	1.2	2.5
Central Kuril	Nov. 15, 2006	8.2	152.25	45.84	30	1.0	0.7
Wenchuan	May. 12, 2008	7.9	103.36	30.99	13	4.7	1.0
Nepal	Apr. 25, 2015	7.8	84.71	28.15	15	1.0	1.2

* Due to plasma bubbles the TEC was much higher.

earthquake induced ionospheric plasma perturbations. The calculation of the ionospheric vertical TEC was done independently at all these sites using both code and phase measurements of the two frequencies, i.e., L1 ($f_1 = 1575.42$ MHz) and L2 ($f_2 = 1227.60$ MHz). Thus, we eliminated the effect of clock errors and tropospheric water vapor and estimated the relative values of slant TEC [18]. Then, the absolute values of TEC are obtained by including the differential satellite biases published by the University of Bern and the receiver bias that are calculated by minimizing the TEC variability between 02:00 and 06:00 LT [19,20]. Thus, estimated TEC can have high degree of accuracy, i.e., at least 10^{14} el/m² at 30 s sampling interval. Short-term ionospheric perturbations are extracted by applying a band-pass filter 2–10 mHz. For representation purpose, we locate the TEC measurement at the intersection of the line of sight and an ionospheric thin layer whose altitude is chosen near the peak of electron density, here at 300 km. These points are referred to as ionospheric piercing points (IPPs).

3. Ionospheric anomalies and implications

The Lithosphere, Atmosphere and Ionosphere (LAI) is a couple system. The first proof of LAI coupling is established following volcanic explosion of Mount Pinatubo in 1991 [21]. The 1964 Mw9.2 Alaska earthquake opened the era of ionospheric seismology [13], by first time detecting earthquake induced ionospheric plasma waves by ionospheric sounding [22]. Though, many large earthquakes occurred after Alaska event, the recent 2004 Mw 9.2 Sumatra and 2011 Mw9.0 Tohoku-Oki earthquakes accompanied by tsunamis generated catastrophic consequences. The later event considered highly instrumentally recorded, in particular with high dense GNSS networks (i.e. GEONET), thus facilitating firm footing to ionospheric seismology. Based on GNSS data, here below, some implications of ionospheric seismology for Indian subcontinent and South-East Asia region are discussed.

3.1. Nepal earthquake and Rayleigh wave group velocity for Indian subcontinent

The collision process of Indian and Eurasian plates has resulted in the creation of the Himalayan range. From the GNSS measurements, the present Indian plate velocity is estimated to be about 50 mm/yr in the ITRF 2005 frame and about 35 mm/yr relative to Eurasian plate [23]. It is widely accepted that various plates driving forces imposing the first-order lithospheric stress perturbations including Gravitational Potential Energy (GPE) deviatoric stress field are responsible for causing the earthquake in Himalaya collision region [24,25]. Thus Himalaya region in Indian subcontinent is prone to large damaging earthquake. Mw7.8 Nepal earthquake occurred on 25 April 2015 (Table 1), also known as the Gorkha earthquake. The seismic moment estimated is 8.1×10^{20} Nm and mainly ruptured SEE region with respect to epicenter. The integrated seismic source model of this earthquake is given by Yagi and Okuwaki [26].

The GNSS data at about 60 sites from various GNSS networks have been used in the present study (Fig. 1). Stacked

ionospheric TEC response at these GPS sites for PRN 23 is also shown in Fig. 1. As seen from the Fig. 1, all the sites within epicentral distance of about 2400 km and 70°–170° azimuth recorded the Rayleigh wave induced TEC response, while the sites within about 400–2200 km in the same azimuth recorded the response from both SAW and RAW. The maximum coseismic-induced peak-to-peak TEC amplitude is about 1.2 TECU. From Hodochron plot [9,27], the apparent Rayleigh wave velocity has been determined as about 2400 ms⁻¹ on the average and the acoustic wave velocity as 1180 ms⁻¹, both these waves being discernible beyond about 1200 km of epicentral distance as also evident from Hodochron plot and wavelet spectrographs [9]. In order to image the Rayleigh group velocity, we considered the Rayleigh wave induced ionospheric response at various permanent GPS sites. Using arrival times of the TEC wave forms, we determined the apparent Rayleigh waves group velocities by cross-correlating the TEC response between any two sites.

The obtained mean group velocity of 2.4 km/s is validated by a global map of Rayleigh group velocities [28]. On the other hand, we have Rayleigh group velocity distribution for Indian subcontinent (for 10–70 s period) estimated from 1001 [29] to 4054 [30] source–receiver paths. Our average group velocity estimated for Bengal Basin, NE and Andaman region has a very good comparison with that of Acton et al. [30] (Fig. 2). These regions show extremely low velocities (about 2100 ms⁻¹) due to the thick sediment blanket [9]. On the other hand, the Indian shield is characterized by high group velocities (about 3900 ms⁻¹) and comparatively lower velocities beneath the Indo Gangetic Plains (IGP) (due to alluvium) and the Himalaya region (due to the thickened crust). Estimation of Rayleigh wave velocity distribution from seismo-ionospheric response is an important step in ionospheric seismology and, in this context, we refer the work of Occhipinti et al. [5] titled ‘the radar that wanted to be a seismometer’ whereby the radar can be a GPS receiver as well.

3.2. Acoustic resonance

The phenomenon of resonant acoustic coupling between the solid earth and the atmosphere occurs when the frequencies of the solid earth modes (seismic hum) overlap the fundamental modes of the atmosphere (atmospheric hum). This condition facilitates triggering of oscillatory acoustic perturbations by ground excitation and vice versa [31]. Resonant oscillations are observed at two frequencies: one is the fundamental Rayleigh wave at periods around 270 s (${}_0S_{29}$) and the other one is the Rayleigh wave at periods around 230 s (${}_0S_{37}$). These frequencies are termed fundamental acoustic resonance frequencies. Nawa et al. [32] first reported the evidence earth's free oscillations, mainly the fundamental spheroidal modes in a frequency range from 0.3 to 5 mHz, based on the superconducting gravimeter data at Syowa Station, East Antarctica. Rolland et al. [33] confirmed the existence of these frequencies during their study of the great Tohoku earthquake.

From the focal mechanism (Fig. 3), it is seen that the 2012 Indian Ocean earthquake are strike slip in nature. Astafyeva

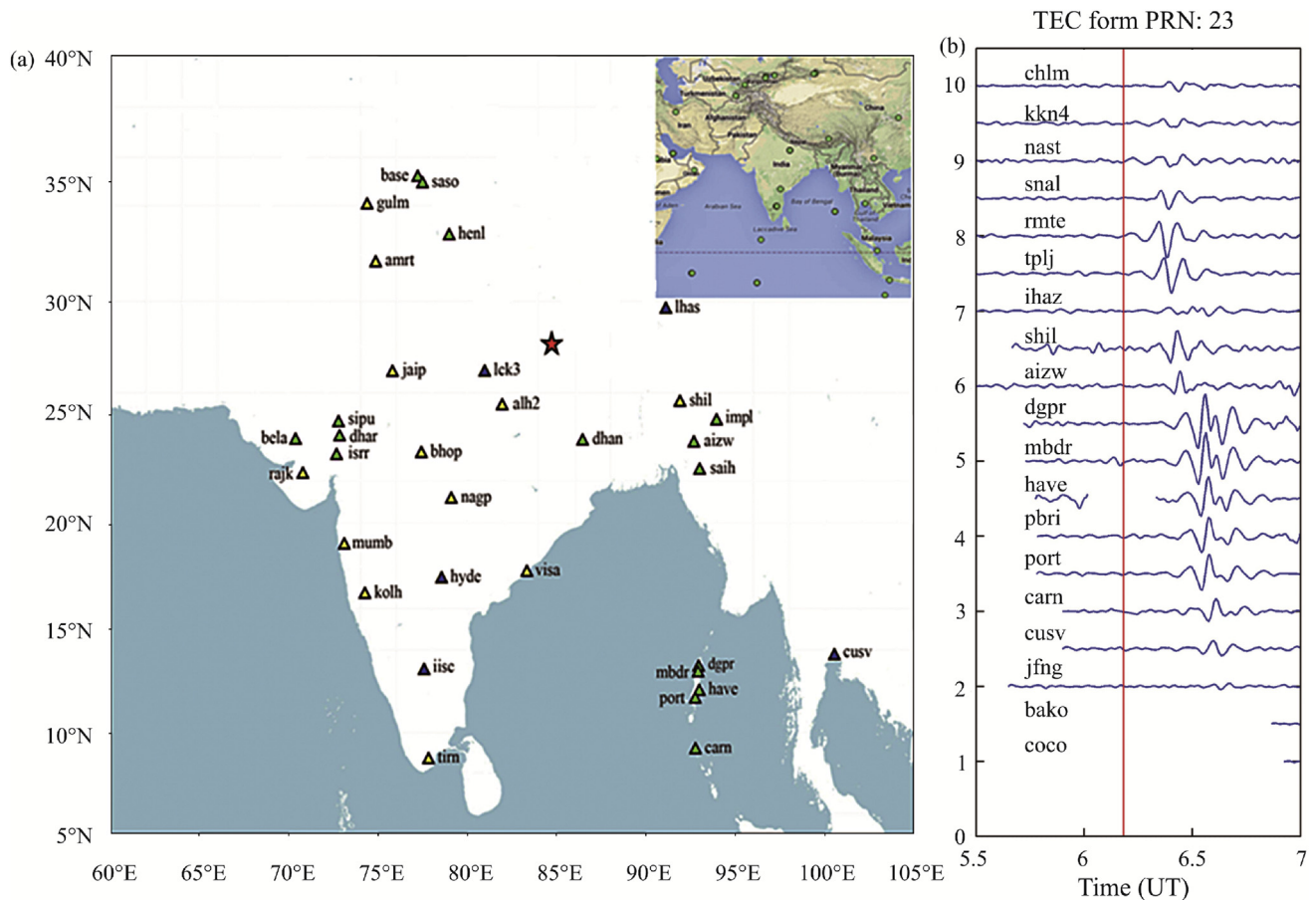


Fig. 1 – a – GPS sites whose data have been analyzed are shown by triangles. The inset gives other IGS sites considered for the study. The red star indicates location of the Mw7.8 Nepal earthquake on April 25, 2015. b – Stacked ionospheric TEC response at various GPS sites for PRN 23. The vertical red line indicates the time of the earthquake.

et al. [34] demonstrated that the strike-slip earthquakes can also be detected in the ionosphere and we can see significant ionospheric response following Mw8.6 event (Fig. 3). The GPS site umlh at about 524 km away from the epicenter exhibited acoustic resonance, observed for a duration of about 1 h after the first earthquake. The wavelet spectrogram of the TEC time series for this site clearly indicated acoustic resonance at 4.0 mHz as seen in Fig. 4, while the top panel shows the dTEC between 09:15 UTC and 10:30 UTC.

By using GEONET GPS data, Rolland et al. [33] have analyzed the ionosphere plasma response to the Mw9.0 Tohoku-Oki earthquake of March 11, 2011. From wavelet spectrogram of the TEC time series at the site 0979 for the PRN 15, they clearly delineated two signals that oscillate with frequencies close to the two fundamental acoustic resonance frequencies (ω_{S29} and ω_{S36}) at about 3.7 and 4.4 mHz. These trapped modes found to have the angular orders smaller than 170 and wavelength larger than about 235 km, and quality factors about 150 and 20 respectively. It should be noted that higher the quality factor, lower the attenuation, hence the resonance last for longer duration [35]. Further, when the seismic source is located in the solid earth, the coupling between the solid part and the atmosphere transfers only $10^{-4} - 10^{-5}$ of the

energy [1,35]. On the other hand, in case of acoustic resonance conditions, it can be 5×10^{-4} of the energy, and LAI is best coupled with good seismic impedance [1]. Another interesting observation seen in Fig. 4 is that a train of wave packet of TEC variation. This phenomenon appears resulting from the beat of the atmospheric modes around observed resonant frequency. Such phenomenon was also seen in 2004 Sumatra earthquake, which is explained by Dautermann et al. [31] and consistent with numerical model by Mastumura et al. [36].

3.3. Tsunami detection by GNSS

Tsunamis are caused by earthquakes or volcanic eruptions under the sea. In open sea, the velocity and amplitude of the tsunami are 700–1000 km/h and 0.1–1 m. Detecting the tsunami response in the ionosphere is valuable signature for tsunami warning system. Scientists are constantly trying and exploring the new ways in monitoring and predicting tsunamis. Some of the organizations continuously monitoring the tsunamis are: Pacific Tsunami Warning Center (PTWC), Hawaii, West Coast & Alaska Tsunami Warning Center (ATWC), Alaska, Indian National Center for Ocean Information Services (INCOIS), India. Here we examine the ionospheric plasma response for tsunami warning from GNSS observations.

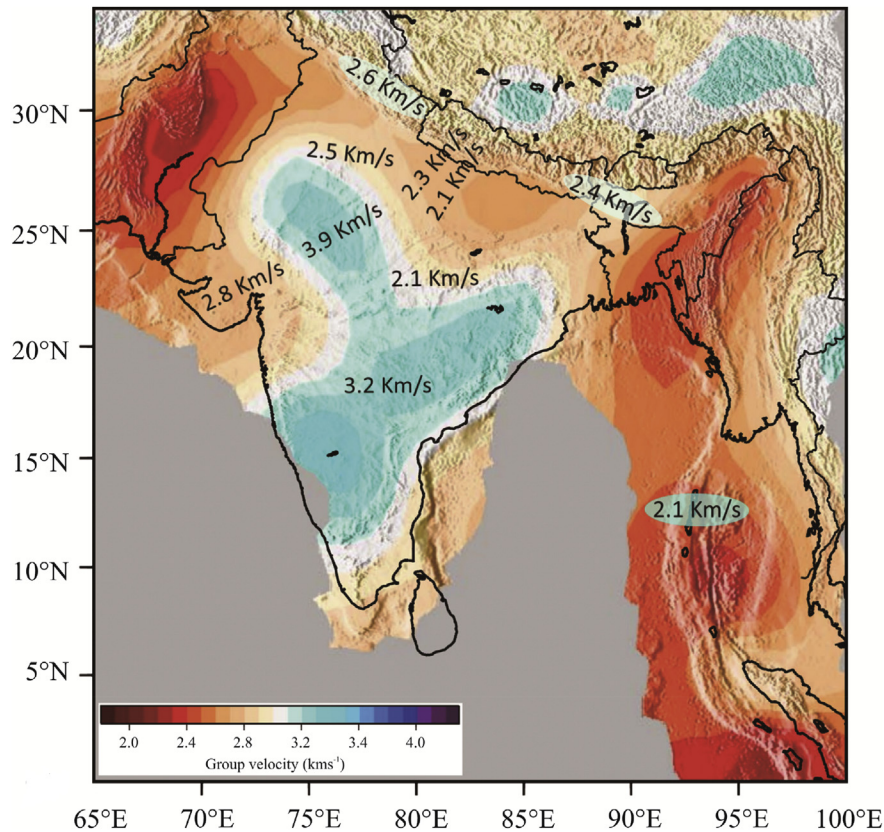


Fig. 2 – The Rayleigh velocities calculated from TEC wave forms are marked on the corresponding region for comparison with Rayleigh wave fundamental group velocity for 10 s obtained by Acton et al. [30] (Reddy et al. [9]).

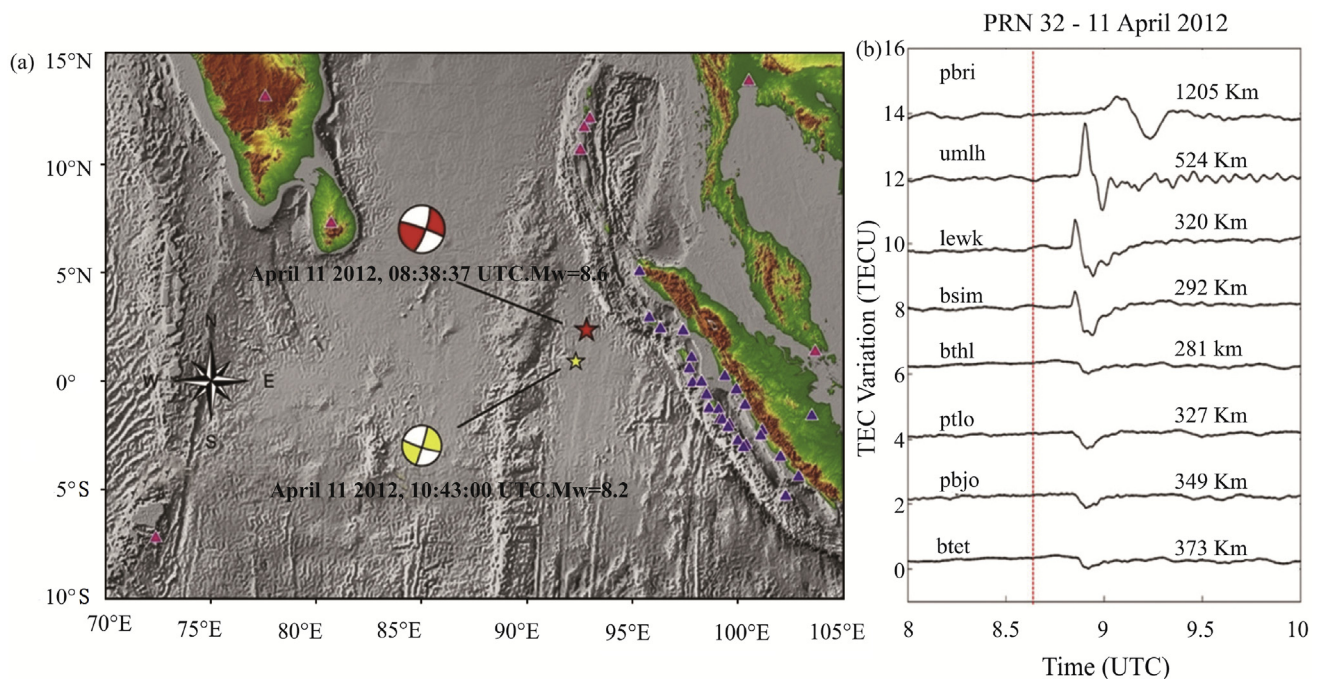


Fig. 3 – a – The red and yellow stars indicate the locations of Mw8.6 and Mw8.2 earthquakes occurred on April 11, 2012 with two hours duration gap. Locations of GPS receiver stations are shown by blue and red triangles indicating SuGAR and IGS GPS stations respectively. b – TEC variations at different GPS sites of SuGAR and IGS networks for PRN 32, between 08:00 and 10:00 UTC on 11 April 2012.

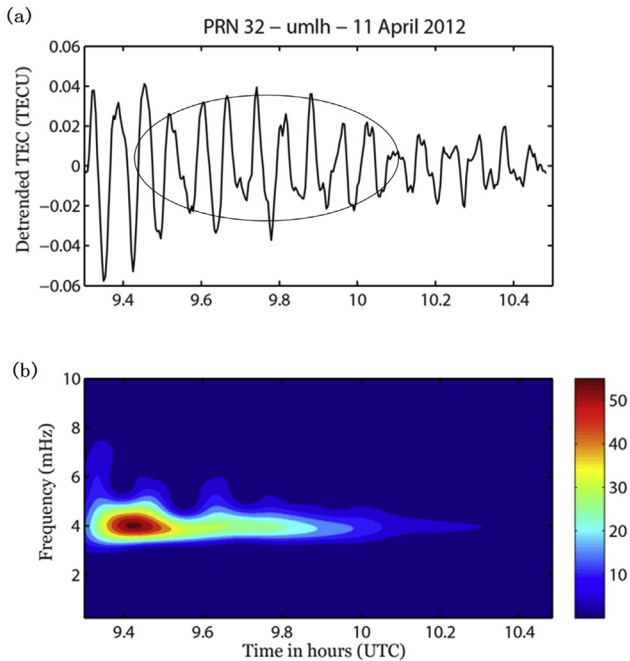


Fig. 4 – Following the 2012 Mw8.6 Indian Ocean event, the acoustic resonance frequency observed in TEC time series at the GPS site ‘umlh’. a-A train of wave packet of TEC variation (enveloped by ellipse) is seen resulting from the beat of the atmospheric modes. b- The wavelet frequency spectrum indicating the resonant frequency at 4.0 mHz [37].

In the open sea, vertical displacement of sea water due to Tsunami can be source of acoustic gravity waves in the atmosphere. These long period gravity waves have frequency smaller than the atmospheric Brunt–Vaisala frequency. The idea that tsunamis produce such waves that are detectable by ionospheric sounding, was theoretically predicted by Hines [38] and Peltier and Hines [39]. Tsunami as propagates, due to dynamic coupling, a fraction of its energy is transferred to the atmosphere in the form of acoustic gravity waves. Atmosphere acts as filter and allows only the long wave length perturbation. This wave propagates with horizontal velocity about 200 ms^{-1} and vertical velocity about 50 ms^{-1} . Due to dynamic coupling, the horizontal velocity matches the speed of the tsunami.

On the other hand, the shock acoustic waves (generated by vertical displacement of terrestrial surface in the epicentral region of an earthquake) induced ionospheric response will reach the 8–10 min after the earthquake and have horizontal velocity $700\text{--}1200 \text{ ms}^{-1}$, i.e. about 4 times faster than that of tsunami. The tsunami waves in the sea created ripples in the ionosphere. Early warning is possible because the disturbances in the ionosphere travel much faster than tsunamis (about four times faster). High dense GNSS receivers can detect the ionospheric disturbances induced by the tsunami waves. Though, Artru et al. [40] detected gravity waves induced by tsunamis similar to Traveling Ionospheric Disturbances (TIDs), the giant tsunami following the 2004 Mw9.2 Sumatra earthquake provided an opportunity and impetus to explore ionospheric tsunami detection using GNSS networks.

The Tohoku-Oki Mw9.0 earthquake of March 11, 2011 earthquake generated a tremendous tsunami with catastrophic consequence with its imprints in the ionospheric plasma, extensively covered and estimated by GEONET GNSS network. This data set while providing a clear image of the rupture characteristics, provided perspective view of tsunami generated gravity waves propagating in the ionosphere. The velocity of gravity waves matched the speed of the tsunami ($200\text{--}300 \text{ m/s}$). From the propagation times of ionospheric disturbances and tsunami waves, the lead times were provided. As the ionospheric perturbation is modulated by the magnetic field inclination, it dithers the estimation of ground displacement (pertaining to Section 3.1) and sea surface displacement [13]. Nevertheless, the ionospheric seismology is a promising tool in augmenting the existing tsunami warning systems.

4. Conclusions

GNSS technology strongly affirmed its potential in providing spatio-temporal perceptives of the large earthquakes, by monitoring their manifestations in ionospheric plasma. At present, many dense GNSS networks, while providing inter-seismic, coseismic and postseismic deformation, also facilitating the insights on the earthquake magnitude, mechanism, rupture process and radiation pattern, thus making possible the ionospheric seismology a reality. Further, it is possible to estimate the Rayleigh group velocity distribution from the ionospheric response to any large earthquake (as it is done for 2015 Nepal event), thereby demonstrating the sensitivity of the ionosphere to crustal inhomogeneities. This is construed as one way of providing authentication of our seismo-ionospheric TEC response. GNSS also contributing to the tsunami disaster mitigation because it has a potential of knowing ionospheric response of the earthquake 10–15 min after the earthquake. This is useful for some regions of South–East Asia, i.e. NE Japan, Indonesia and Indian coastal regions where tsunami takes 0.5–2 h to reach the coast. The imaged ionospheric perturbations from dense GNSS networks could, in principle, be used as a proxy to study the coupling and energy transfer processes in the Lithosphere, Atmosphere and Ionosphere (LAI) coupled system.

Acknowledgments

Author thanks ISGN team at INCOIS for providing the GNSS data. Sincere efforts by all our magnetic observatory staff who are maintaining the GNSS receivers gratefully acknowledged. I thank D.S. Ramesh (Director, IIG) for giving impetus in ionospheric seismology studies in our institute. The author thanks the reviewers for their valuable comments and suggestions for improving this paper.

REFERENCES

- [1] Lognonné P, Garcia R, Crespon F, Occhipinti G, Kherani A, Artru-Lambin J. Seismic waves in the ionosphere. *Europhys News* 2006;37(4):11–4.

- [2] Liu JY, Tsai YB, Chen SW, Lee CP, Chen YC, Yen HY, et al. Giant ionospheric disturbances excited by the M9.3 Sumatra earthquake of 26 December 2004. *Geophys Res Lett* 2006;33:L02103. <http://dx.doi.org/10.1029/2005GL023963>.
- [3] Ogawa T, Nishitani N, Tsugawa T, Shiokawa K. Giant ionospheric disturbances observed with the Super DARN Hokkaido HF radar and GPS network after the 2011 Tohoku earthquake. *Earth Planets Space* 2012;64:1295–307.
- [4] Liu JY, Chen YI, Huang CC, Parrot M, Shen XH, Pulnits SA, et al. A spatial analysis on seismo-ionospheric anomalies observed by DEMETER during the 2008 M8.0 Wenchuan earthquake. *J Asian Earth Sci* 2015;114:414–9.
- [5] Occhipinti G, Dorey P, Farges T, Lognonne P. Nostradamus: the radar that wanted to be a seismometer. *Geophys Res Lett* 2010;37:L18104. <http://dx.doi.org/10.1029/2010GL044009>.
- [6] Coisson P, Occhipinti G, Lognonne P, Rolland LM. Tsunami signature in the ionosphere: the innovative role of OTH radar. *Radio Sci* 2011;46:RS0D20. <http://dx.doi.org/10.1029/2010RS004603>.
- [7] Heki K. Ionospheric electron enhancement preceding the 2011 Tohoku-Oki earthquake. *Geophys Res Lett* 2011;38:L17312. <http://dx.doi.org/10.1029/2011GL047908>.
- [8] Jin SG, Jin R, Li JH. Pattern and evolution of seismo-ionospheric disturbances following the 2011 Tohoku earthquakes from GPS observations. *J Geophys Res Space Phys* 2014;119(9):7914–27.
- [9] Reddy CD, Seemala GK. Two-mode ionospheric response and Rayleigh wave group velocity distribution reckoned from GPS measurement following Mw 7.8 Nepal earthquake on 25 April 2015. *J Geophys Res Space Phys* 2015;120. <http://dx.doi.org/10.1002/2015JA021502>.
- [10] Reddy CD, Shrivastava MN, Seemala G, Gabriel E, Carlos JB. Ionospheric plasma response to Mw8.3 Chile Illapel earthquake on September 16, 2015. *PAAG-D-15-00374R1*. 2016.
- [11] Ducic V, Artru J, Lognonne P. Ionospheric remote sensing of the Denali earthquake Rayleigh surface waves. *Geophys Res Lett* 2003;30(18):1951–4.
- [12] Jin S, Occhipinti G, Jin R. GNSS ionospheric seismology: recent observation evidences. *Earth-Science Rev* 2015;147:54–64.
- [13] Occhipinti G. The seismology of the planet Mongo: the 2015 ionospheric seismology review. In: Morra G, Yuen DA, King S, Lee SM, Stein S, editors. *Subduction dynamics: from mantle to mega disasters*. AGU; 2015.
- [14] Shah M, Jin SG. Statistical characteristics of seismo-ionospheric GPS TEC disturbances prior to global Mw \geq 5.0 earthquakes (1998–2014). *J Geodyn* 2015;92:42–9.
- [15] Cahyadi MN. Near-Field coseismic ionospheric disturbances of earthquakes in and around Indonesia. The Degree of Doctor of Philosophy. Dept. Natural History Sciences, Graduate School of Science, Hokkaido University; 2014.
- [16] Cahyadi MN, Heki K. Coseismic ionospheric disturbance of the large strike-slip earthquakes in North Sumatra in 2012: Mw dependence of the disturbance amplitudes. *Geophys J Int* 2015;200:116–29.
- [17] Dow JM, Neilan RE, Rizos C. The International GNSS Service in a changing landscape of Global Navigation Satellite Systems. *J Geod* 2009;83:191–8.
- [18] Sardón E, Zarraga N. Estimation of total electron content using GPS data: how stable are the differential satellite and receiver instrumental biases? *Radio Sci* 1997;32(5):1899–910.
- [19] Seemala GK, Valladares CE. Statistics of total electron content depletions observed over the South American continent for the year 2008. *Radio Sci* 2011;46:RS5019. <http://dx.doi.org/10.1029/2011RS004722>.
- [20] Valladares CE, Villalobos J, Hei MA, Sheehan R, Basu S, MacKenzie E, et al. Simultaneous observation of travelling ionospheric disturbances in the Northern and Southern Hemispheres. *Ann Geophys* 2009;27:1501–8.
- [21] Kanamori H, Mori J. Harmonic excitation of mantle Rayleigh waves by the 1991 eruption of Mount Pinatubo, Philippines. *Geophys Res Lett* 1992;19:721–4.
- [22] Davies K, Baker DM. Ionospheric effects observed around the time of the Alaskan earthquake of March 28, 1964. *J Geophys Res* 1965;70:2251–3.
- [23] Reddy CD, Sunil PS, Prajapati SK, Ponraj M, Amrithraj S. Geodynamics of the NE Indian lithosphere: geodetic, geophysical and seismo-tectonic, perspective. *Mem Geol Soc India* 2012;77:241–50.
- [24] Shrivastava MN, Reddy CD, Prajapati SK. Topographic constraints on deviatoric stress field in the Indo-Eurasian collision region: seismo-tectonic implications. *Pure Appl Geophys* 2012;170:515–27. <http://dx.doi.org/10.1007/s00024-012-0570-9>.
- [25] Shrivastava MN, Reddy CD. The Mw 8.6 Indian ocean earthquake on April 11, 2012: co-seismic displacement, Coulomb stress change and aftershocks pattern. *J Geol Soc India* 2012;81:813–20.
- [26] Yagi Y, Okuwaki R. Integrated seismic source model of the 2015 Gorkha, Nepal, earthquake. *Geophys Res Lett* 2015;42:6229–35. <http://dx.doi.org/10.1002/2015GL064995>.
- [27] Reddy CD, Sunil AS, González G, Shrivastava MN, Moreno M. Near-field co-seismic ionospheric response due to the northern Chile Mw 8.1 Pisagua earthquake on April 1, 2014 from GPS observations. *J Atmos Solar-Terrestrial Phys* 2015;134:1–8.
- [28] Larson EW, Ekstrom G. Global models of surface wave group velocity. *Pure Appl Geophys* 2001;158:1377–99.
- [29] Mitra S, Priestley K, Gaur VK, Rai SS, Haines J. Variation of Rayleigh wave group velocity dispersion and seismic heterogeneity of the Indian crust and uppermost mantle. *Geophys J Int* 2006;164:88–98.
- [30] Acton CE, Priestley K, Gaur VK, Rai SS. Group velocity tomography of the Indo Eurasian collision zone. *J Geophys Res* 2010;115:B12335. <http://dx.doi.org/10.1029/2009JB007021>.
- [31] Dautermann TE, Calais E, Lognonné P, Mattioli G. Lithosphere- Atmosphere-Ionosphere coupling after the 2003 explosive eruption of the Soufriere Hills Volcano, Montserrat. *Geophys J Int* 2009;179(3):1537–46.
- [32] Nawa K, Suda N, Fukao Y, Sato T, Aoyama Y, Shibuya K. Incessant excitation of the Earth's free oscillations. *Earth Planets Space* 1998;50:3–8.
- [33] Rolland L, Lognonné P, Astafyeva E, Kherani A, Kobayashi N, Mann M, et al. The resonant response of the ionosphere imaged after the 2011 Tohoku-Oki earthquake. *Earth Planet Space* 2011;63:853–7.
- [34] Astafyeva E, Rolland LM, Sladen A. Strike-slip earthquakes can also be detected in the ionosphere. *Earth Planet Sci Lett* 2014;405:180–93.
- [35] Lognonné P, Clévéde E, Kanamori H. Computation of seismograms and atmospheric oscillations by normal-mode summation for a spherical earth model with realistic atmosphere. *Geophys J Int* 1998;135(2):388–406.
- [36] Matsumura M, Saito A, Iyemori T, Shinagawa H, Tsugawa T, Otsuka Y, et al. Numerical simulations of atmospheric waves excited by the 2011 off the Pacific coast of Tohoku earthquake. *Earth Planets Space* 2011;63:885–9.
- [37] Sunil AA, Bagiya MS, Reddy CD, Kumar M, Ramesh DD. Post-seismic ionospheric response to the 11 April 2012 east Indian

Ocean doublet earthquake. *Earth Planets Space* 2015;134:1–8.
<http://dx.doi.org/10.1186/s40623-015-0200-8>.

- [38] Hines CO. Gravity waves in the atmosphere. *Nature* 1972;239:73–8.
- [39] Peltier WR, Hines CO. On the possible detection of tsunamis by a monitoring of the ionosphere. *J Geophys Res* 1976;81(12):1995–2000.
- [40] Artru J, Ducic V, Kanamori H, Lognonné P, Murakami M. Ionospheric detection of gravity waves induced by tsunamis. *J Geophys Res* 2005;160(3):840–8.



C.D. Reddy is a professor at Indian Institute of Geomagnetism, New Bombay, India, leading GNSS studies. His present research interests are Ionospheric Seismology, Silent Earthquakes, Crustal Deformation and Space Weather. His main focus is on Lithosphere Atmosphere, Ionosphere and Magnetosphere (LAIM) coupling processes.